Data Extrapolation Method for The Dynamic Increasing Energy Test: SEM-CASE

E.C. Alves, M.M. Sales, P.M.F. Viana

Abstract. The dynamic increasing energy test has been widely used in pile load tests in Brazil in recent years. However, the ultimate strength of the single-foundation system is not mobilized in most of the tests because of various factors. In some cases, the equipment available cannot attain the necessary kinetic energy, or the structural element presents initial imperfections/ruptures. In this study, the authors present a method for extrapolating the mobilized static resistance *vs.* maximum displacement curve, which is obtained using the dynamic increasing energy test (DIET). Using the force and velocity signals collected by the PDA (Pile Driving Analyzer) system, it is possible to calculate the resistance and displacement by applying the Simplified CASE Method. An extrapolation method, the Simplified Extrapolation Method of the CASE Method (SEM-CASE), is presented based on the results of twenty-one precast concrete pile load tests that have been carried out in different soils. The estimated values of the ultimate complementary energy and ultimate strength were very close to the measured values in the presented load tests.

Keywords: extrapolation method; dynamic load test; driven pile; complementary energy; strain energy.

1. Introduction

The first methods used to estimate the bearing capacity of a driven pile were based on data obtained during the pile installation. Alternatively, the wave equation was initially applied to piles in the 1930s to estimate bearing capacity (Warrington, 1997; Hussein & Goble 2004). Smith (1960) presented a model that used a group of equations and calculation routines to describe the stress-wave displacement and its effects along the pile after a hammer blow. With the development of more powerful sensors and computers, Smith's model can now be applied and has become the fundamental basis for the methods employed in dynamic load test analysis.

In this context, considering the need to estimate the ultimate capacity of the pile based on the dynamic load test, this paper presents a method for extrapolating the mobilized static resistance (R) *vs.* maximum displacement (D) curve to obtain the behavior and ultimate strength capacity of the dynamic increasing energy test (dynamic load test).

The method is used for driven precast concrete piles, which mobilize the shaft and toe resistance during loading. The guiding principle of this method is the complementary energy criterion first presented by Aoki (1997), which uses the expression "mobilized static resistance" to indicate the resistance of the static portion that is mobilized after a hammer blow during the dynamic load test, as calculated by the simplified CASE method.

2. Dynamic Test and Numerical Analysis

2.1. Dynamic load test

The purpose of the dynamic load test is to estimate the ultimate static resistance of the pile-soil system and propose a load *vs.* virtual-settlement curve.

By applying a hammer blow to the head of the pile, generally through a pile driver, force and velocity signals are obtained at the pile head with deformation and acceleration sensors, respectively (Teferra *et al.*, 1996; Likins *et al.*, 2008). The signals obtained from the sensors are transferred to and stored in a portable computer, known as PDA (Pile Driving Analyzer).

After the data have been collected by the sensors, the PDA transcodes and processes the data to obtain the force and velocity signals, and the CASE numerical method provides the static resistance in each hammer blow at the moment of impact during the pile driving.

2.2. Dynamic increasing energy test - DIET

Two types of dynamic load tests can be used to obtain the pile-bearing capacity: constant or increasing energy. The dynamic constant energy test is the most traditional and widely used test worldwide. According to Aoki (1989a), the dynamic constant energy test is similar to a cyclic static load test in which the same load is always applied, and the same settlement is always obtained for the same strain energy.

Eder Chaveiro Alves, M.Sc., Civil Engineering, Agência Goiana de Transporte e Obras, AGETOP. Av. Gov. José Ludovico de Almeida, n° 20, 74775-013 Goiânia, GO, Brazil. e-mail: ederchaveiro@yahoo.com.br.
Maurício Martines Sales, Ph.D., Associate Professor, Escola de Engenharia Civil e Ambiental, Universidade Federal de Goiás, UFG. Praça Universitária, 1488, 74605-220 Goiânia, GO, Brazil. e-mail: sales.mauricio@gmail.com.
Paulo Márcio Fernandes Viana, Ph.D., Associate Professor, Departamento de Engenharia Civil, Universidade Estadual de Goiás, UEG. BR-153, Quadra área, km 99, 75132-903 Anápolis, GO, Brazil. e-mail: pmfviana@gmail.com.
Submitted on July 15, 2015; Final Acceptance on March 3, 2016; Discussion open until December 30, 2016.

The increasing energy test consists in the application of blows with variable and increasing fall heights, based on a level of energy that is lower than that of the driving end (free-fall impact system) (Aoki, 2000). Currently, the increasing energy method is the most frequently used method for performing the dynamic load test in Brazilian building foundations.

Aoki (1989a) presents the application of the dynamic increasing energy test to obtain a curve similar to the load *vs.* settlement curve obtained in the static load test, which is the mobilized static resistance *vs.* displacement curve.

2.3. Simplified CASE method

Developed by the Case Institute of Technology (currently Case Western Reserve University), the main objective of this method is to calculate the static resistance in real time and at the test site for each hammer blow. It was implicit that each blow was enough to mobilize the ultimate soil resistance.

This method is a closed-form solution of the wave equation, in which the signals of force and velocity are used and recorded in a particular pile section, just as the blow reaches its highest intensity in the section of the sensors (t_1) and just as the wave reflected at the end of the pile returns to the instrumented section (t_2).

Static resistance (R) is calculated by the difference between total resistance and dynamic resistance. Linkins & Rausche (1981) presented the start point of Case Method and in following paper, Rausche *et al.* (1985) expanded the formulation of static resistance as

$$R=\frac{(1-Jc)\times\left[Ft_1+\left(\frac{EA}{c}\right)vt_1\right]+(1+Jc)\times\left[Ft_2-\left(\frac{EA}{c}\right)vt_2\right]}{2} \quad (1)$$

where Ft_1, Ft_2, vt_1, and vt_2 are, respectively, the values of force and velocity calculated by means of the data obtained through the specific deformation and acceleration sensors at times t_1 and t_2. Jc is a dimensionless constant called the "dynamic damping coefficient" of the CASE method and is determined based on experiences of correlations with static load test results, E is the elastic modulus of pile material, A is the cross-sectional area of pile and c is the velocity of wave propagation. The relation (EA/c) is also known as the pile impedance.

3. Complementary Energy

Presented by Aoki (1989b), this criterion allows the pile-soil system to be in a state of dynamic equilibrium (elastic-perfectly plastic behavior) during the hammer impact, with the appearance of non-conservative inertial and damping forces, and the application of Hamilton's energy conservation principle is valid. It is also assumed that the system returns to its original state after each blow, *i.e.*, there is no significant change in the initial condition of the system. Clough & Penzien (1975) stated the principle as:

$$\int_{t_1}^{t_2}\delta(T-V)dt+\int_{t_1}^{t_2}\delta(W_{nc})dt=0 \quad (2)$$

where δ is the variation in the time interval (t_2 - t_1); T is the total kinetic energy in the system; V is the potential energy in the system; W_{nc} is the work done by non conservatives forces.

Soil rupture is characterized in the dynamic increasing energy test when a particular impact, corresponding to a point on the idealized mobilized static resistance-displacement curve, shows that a) the mobilized static bearing capacity (R) passes through a maximum R_u; b) the complementary kinetic energy (T_c) of the impact passes through a maximum T_{cu}; and c) the complementary potential energy (V_c) passes through a maximum V_{cu}.

Hamilton's principle, as applied to the maximum impact energy T_u, also can be expressed by

$$\{[T_u-(R_u\times K_u)/2]-[(R_u\times S_u)+W_{au}]\}=0 \quad (3)$$

where T_u is the maximum kinetic energy; S_u is the maximum permanent portion (penetration); and W_{au} is the work done by the non conservative forces.

The complementary energy V_c tends towards a constant value V_{cu} when the total strain energy V and the settlement S tend towards infinity, *i.e.*, the analysis of the variation of the complementary strain energy with loading shows how close rupture is because the rate of variation of this parameter is cancelled out when the reaction or resistance capacity of the system reaches an extreme, as shown in Fig. 1.

Aoki (2000) presented the new formulations for determining the values of potential energy V_s, complementary energy V_c, and work W done by the static portion of the forces. These made it possible to calculate area values that are more consistent with the mobilized static resistance (R) *vs.* displacement (D) curve. The expressions are given below for calculating the potential energy (Eq. 4), complementary energy (Eq. 5), and work (Eq. 6):

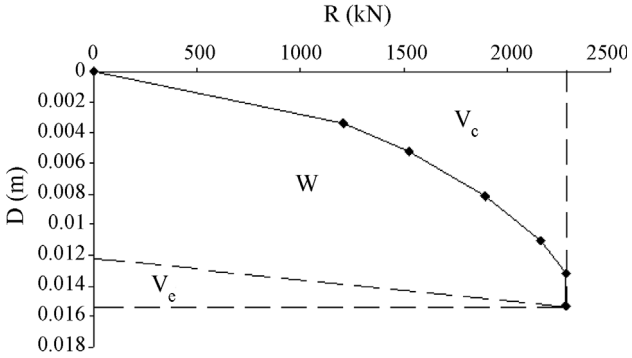

Figure 1 - The strain energies that form part of the mobilized static resistance (R) *vs.* maximum displacement (D) curve of DIET.

$$V_s = \sum_{i=1}^{n}\left(\frac{R_i + R_{i+1}}{2}\right)\times(D_i - D_{i-1}) \quad (4)$$

$$V_c \cong RD - \sum_{i=1}^{n}\left(\frac{R_i + R_{i+1}}{2}\right)\times(D_i - D_{i-1}) \quad (5)$$

$$W = (V_s - V_e) \quad (6)$$

where V_e is the portion of elastic strain energy (Fig. 1).

4. Fit Equations for *"R vs. D"* Curve

This section presents the use of the exponential, hyperbolic, and parabolic functions as possible models to represent the mobilized static resistance (*R*) *vs.* Displacement (*D*) curve, as shown in Fig. 2. Moreover, the equations for the calculation of complementary energy (V_c) were deduced by means of Eqs. 7 to 15 (see all detailing in the appendix), which present different approaches to represent the mobilized static resistance (*R*) *vs.* displacement curve, the complementary energy (V_c), and the ultimate complementary energy (V_{cu}), using the ultimate static resistance R_u and displacement (D_u) at the moment that the test mobilizes the ultimate static resistance. The other variables presented in this figure are: D_1 and D_2 are displacements before and after the ultimate static resistance, respectively; ΔD_1 and ΔD_2 are displacement variations; R_1 is the static resistance corresponding to a displacement "D_1"; ΔR is a static resistance variation; *V* is the potential energy; ΔV_1 and ΔV_2 are energy variations; ΔV_{c1} is the corresponding variation in the complementary energy.

- Exponential curve

$$R = R_u(1 - \exp^{-(\alpha D)}) \quad (7)$$

$$Vc = \left(\frac{R_u}{\alpha}\right)[1 - (1 + \alpha D)\exp^{-\alpha D}] \quad (8)$$

$$V_{cu} = \frac{R_u}{\alpha}. \quad (9)$$

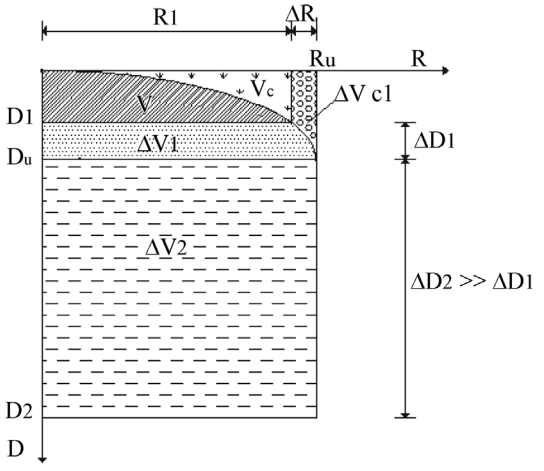

Figure 2 - Mobilized static resistance (*R*) *vs.* maximum displacement(*D*) curve of DIET (modified from Aoki, 2000).

- Hyperbolic curve

$$R = R_u\sqrt{1 - \left(1 - \frac{D}{D_u}\right)^2} \quad (10)$$

$$V_c = (R \times D_u) - \left(\frac{D_u}{R_u}\right)\left[\frac{R}{2}\sqrt{R_u^2 - R^2} + \frac{R_u^2}{2}\,arcsen\left(\frac{R}{R_u}\right)\right] \quad (11)$$

$$V_{cu} = 0{,}215 \times R_u \times D_u. \quad (12)$$

- Parabolic curve

$$R = \sqrt{R_u^2\left(\frac{D}{D_u}\right)} \quad (13)$$

$$V_c = D_u\left(\frac{R^3}{3R_u^2}\right) \quad (14)$$

$$V_{cu} = \frac{(D_u \times R_u)}{3}. \quad (15)$$

5. SEM-CASE Method

A new method is presented here for extrapolating the trajectory of the mobilized static resistance (*R*) *vs.* maximum displacement (*D*) curve, obtained by analyzing the CASE numerical method based on the complementary energy criterion. This methodology is hereafter called the Simplified Extrapolation Method of the Simplified CASE Method (SEM-CASE).

This method is applicable to precast concrete piles driven by a pile driver with a free-fall hammer and tested by the dynamic increasing energy test. In addition, the pile must have been designed to bear the working load using the portions of shaft and toe resistance, where the rupture is characterized by constant mobilized static resistance under the action of increasing kinetic energy with a well-defined vertical asymptote.

Some pile tests can present different forms of "resistance *vs.* displacement" curves. Sometimes the tests do not present an evident mobilization of static resistance. In others, the results are initially represented by an almost linear behavior in the graph *R* x *D* and then occurs an abrupt "failure". Both cases are consequences of particular pile-soil systems and can not be extrapolated or predicted by any method. Aoki (2000) discussed some examples of pile tests in such cases. The "SEM-CASE" method will not be able to extrapolate the maximum static resistance in such curves.

The data from a dynamic increasing energy test presented by Aoki (2000) were used to demonstrate the use of the method (Fig. 3). The concrete pile had a total length of 12 m, a driven length of 10.1 m, a diameter of 0.42 m, and a hollow cylindrical form with a section area of 0.09 m^2.

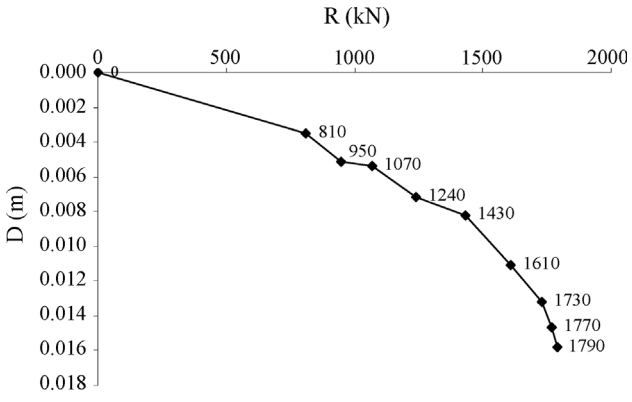

Figure 3 - R *vs. D* graph of a driven pile (modified from Aoki, 2000).

This pile reached the ultimate resistance during the test, according to the complementary energy criterion. However, to simulate a dynamic load test that did not mobilize the ultimate static resistance, Fig. 3 represents only part of the test as if it had been interrupted when the resistance reached 1790 kN (the other points beyond 1790 kN are not presented in Fig. 3).

The application of the method can be divided into three (3) steps:

- **Step 01**: The variation ratio of the mobilized static resistance (*Var. R*) to the variation of kinetic energy (*Var. T*) is calculated in each blow of the dynamic load test. The values obtained for the pile are shown in Table 1. The values for the ratio of *Var. R* to *Var. T* are plotted in Fig. 4, with the values of the mobilized static resistance *R* plotted on the abscissa using a logarithmic scale.

The graph in Fig. 4 has three (3) stages: Stage 1, Stage 2, and Stage 3.

Stage 1 has an almost 90° slope in relation to the *x*-axis. The first blows, with a lower fall height, *i.e.*, lower kinetic energy, generally form part of this stage.

Stage 2 has a slope tending from 90° to 0°, in relation to the x-axis, depending on the analyzed pile. Stage 3 tends to a 90° slope, regardless of the analyzed pile geometry.

The slope of the three stages of the *R vs. Var. R*/ *Var. T* graph varies according to the following characteristics of the pile foundation: a) Local surrounding soil; b) Pile geometry; c) Length of the structural element driven into the surrounding soil; and d) "Pile age" (time interval between the end of the driving and the start of the test).

From analyses of the 21 dynamic increasing energy tests studied by Alves (2010), it was observed that in stage 1, the test practically mobilizes only the lateral resistance. In stage 2, the test mobilizes the lateral and tip resistance of the pile, and in stage 3, the lateral resistance during the test is "exhausted" (remains constant), and only the tip resistance increases continuously and is mobilized until rupture (when the ratio of the variation of the mobilized static resistance - *Var. R* to the variation in applied kinetic energy - *Var. T* is equal to zero), indicating similarities with the results presented by Aoki (1989b).

Figure 5 uses the last five points, which are in stage 3 of Fig. 4, to present a simple linear regression. It shows good agreement between the points and the linear regression. This good agreement occurs when the portion of tip resistance of the pile is "significantly" mobilized.

The principle of extrapolation of the ultimate static resistance stems from the concept that when the ratio (*Var. R*/*Var. T*) is equal to zero, the pile reaches the ultimate resistance, *i.e.*, when the variation of the mobilized static resistance in two blows with increasing kinetic energy is equal to zero, the pile is subject to the mobilization of the ultimate static resistance. As stated by Aoki (2000), this kind of approach would be the upper boundary limit of the ultimate static resistance.

Figure 5 shows the linear regression of the points that is used to extrapolate the ultimate static resistance (R_u). This occurs when the straight line intercepts the *x*-axis.

Table 1 - Values of *D*, *R*, *T*, *Var. R*, *Var. T*, and *Var. R*/*Var. T*.

D (m)	*R* (kN)	*T* (kNm)	*Var. R* (kN)	*Var. T* (kNm)	*Var. R*/*Var. T* (1/m)
0	0	0	0	0	0
0.0035	810.0	1.9	810.0	1.9	426.32
0.0051	950.0	3.0	140.0	1.1	127.27
0.0054	1070.0	3.9	120.0	0.9	133.33
0.0072	1240.0	5.8	170.0	1.9	89.47
0.0082	1430.0	7.3	190.0	1.5	126.67
0.0111	1610.0	11.8	180.0	4.5	40.00
0.0132	1730.0	15.9	120.0	4.1	29.27
0.0147	1770.0	18.6	40.0	2.7	14.81
0.0158	1790.0	21.1	20.0	2.5	8.00

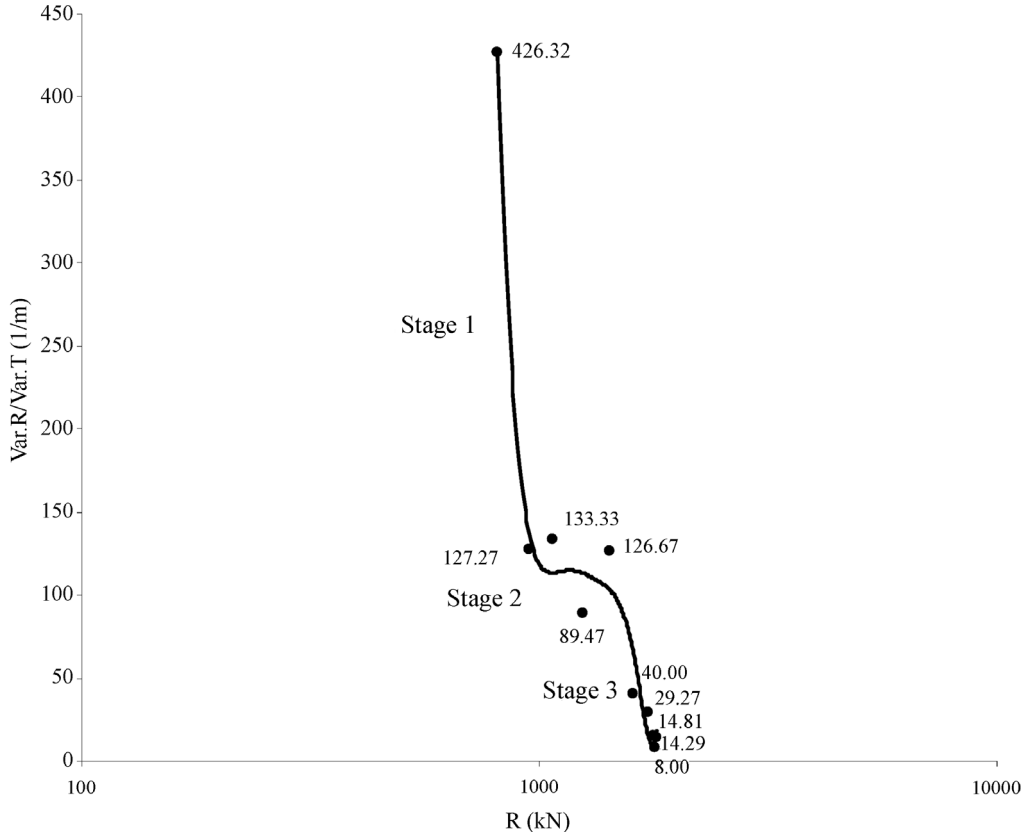

Figure 4 - R *vs. Var. R/ Var.T* graph of a driven pile.

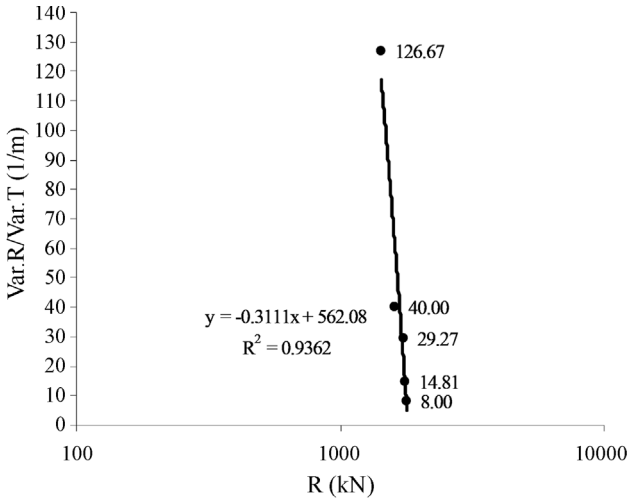

Figure 5 - Linear regression of the last five points of the *R vs. Var. R/Var. T* graph of a driven pile.

The linear regression expression is described below

$$y = ax + b \tag{16}$$

$$R_u = -\frac{b}{a}. \tag{17}$$

Note that the correlation coefficient (R^2) had a value of 0.9362. According to the studies of Alves (2010), values greater than 0.8 were found in all tests. Solving the linear regression expression in Fig. 5, an estimated ultimate static resistance value of 1806.8 kN can be obtained. Therefore, the extrapolated ultimate mobilized static resistance R_u is determined by Eq. 17.

- **Step 02:** The *R* x *D* curve in Fig. 3 is divided into equal maximum displacement segments (Fig. 6). The recommended division value is 1 mm, as used in this example. The values of mobilized static resistance – R_n are calculated by means of interpolation. This task produces a smoother curve in the segments where it has sudden variations in trajectory. The complementary energy values are calculated in each segment as

$$V_{cn} \cong \sum_{n=1}^{i}\left(\frac{D_n + D_{n-1}}{2}\right)\times(R_n - R_{n-1}). \tag{18}$$

Table 2 presents the values for maximum displacement adopted (D_n) for the interpolated mobilized static resistance (R_n) and the calculated values, with Eq. 18, and for the complementary energy in the analyzed segment (Vc_n) of the test.

The values of Vc_n *vs.* Vc_{n-1}, presented in Table 2, are plotted in Fig. 7. After the quadratic regression of the plotted points, this regression was extrapolated until it inter-

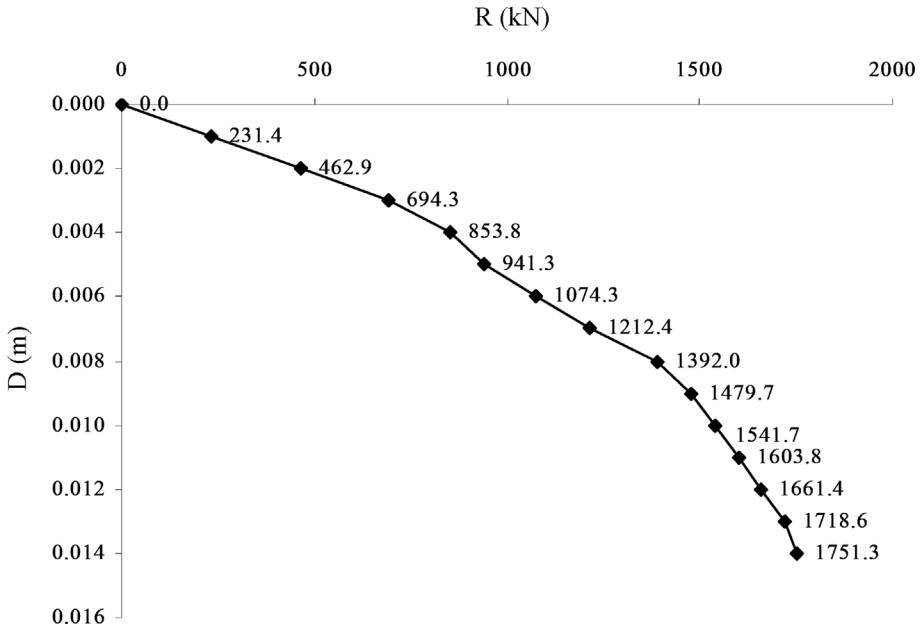

Figure 6 - *R vs. D* graph divided into equal maximum displacement segments.

Table 2 - Interpolated *D* and *R* values and the calculated *Vc*.

D (m)	R_n (kN)	R_{n-1} (kN)	Vc_n (kNm)	Vc_{n-1} (kNm)
0.0000	0.00	-	0.00	-
0.0010	231.43	0.00	0.12	0.00
0.0020	462.86	231.43	0.46	0.12
0.0030	694.29	462.86	1.04	0.46
0.0040	853.75	694.29	1.60	1.04
0.0050	941.25	853.75	1.99	1.60
0.0060	1074.29	941.25	2.72	1.99
0.0070	1212.38	1074.29	3.62	2.72
0.0080	1392.00	1212.38	4.97	3.62
0.0090	1479.66	1392.00	5.71	4.97
0.0100	1541.72	1479.66	6.30	5.71
0.0110	1603.79	1541.72	6.96	6.30
0.0120	1661.43	1603.79	7.62	6.96
0.0130	1718.57	1661.43	8.33	7.62
0.0140	1751.33	1718.57	8.78	8.33
0.0150	1776.92	1751.33	9.15	8.78

cepted the dotted line. The dotted line represents the points at which the values of Vc_n are equal to those of Vc_{n-1}, *i.e.*, a situation in which, under the complementary energy criterion, the test would mobilize the ultimate static resistance.

The quadratic equation, according to Eq. 19, is used to determine the ultimate complementary energy (V_{cu}) when the pile reaches its rupture point.

$$ax^2 + (b-1)x + c = 0. \quad (19)$$

The values of "*a*", "*b*", and "*c*", as found in the quadratic regression (Fig. 7), are substituted into Eq. 19. The unknown quantity "*b*" is reduced by 1 to arrive at the condition where both axis values are equal, *i.e.*, Vc_n is equal to Vc_{n-1}.

Solving the quadratic equation, Vc_{u1} and Vc_{u2} are found, discarding any Vc_u value that eventually is negative or has no physical significance.

In the example presented here, by solving the equation shown in Fig. 7, a Vc_u value of 10.06 kN is found.

- **Step 03:** Using the values obtained for the ultimate mobilized static resistance and for the ultimate complementary energy of the test, it is possible to extrapolate the remaining segment of the mobilized static resistance (*R*) *vs.* maximum displacement (*D*) curve. Eqs. 7 to 15 can be used for this purpose.

Finally, by substituting the values Vc_u = 10.06 kJ and R_u = 1806.8 kN into Eq. 9, Eq. 12 and Eq. 15, the parameters for the exponential, hyperbolic, and parabolic equations, respectively ($\alpha \approx 1179.6$, $D_u \approx 0.0259$ m, and $D_u \approx 0.0167$ m), can be obtained.

Figure 8 shows the comparison of the mobilized static resistance (*R*) x maximum displacement (*D*) curve measured in the dynamic increasing energy test with the curves calculated by the exponential, hyperbolic, and parabolic equations.

6. Results and Discussions

6.1. Analyzed tests

The dynamic load tests were carried out starting with the application of increasing dynamic axial loads, using a free fall hammer, in different Brazilian states.

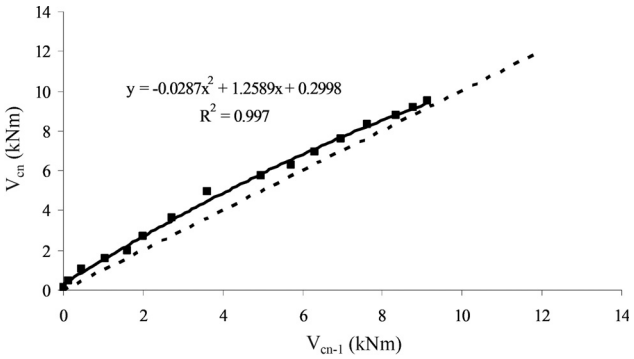

Figure 7 - Vc_{n-1} *vs.* Vc_n graph of a driven pile with quadratic regression.

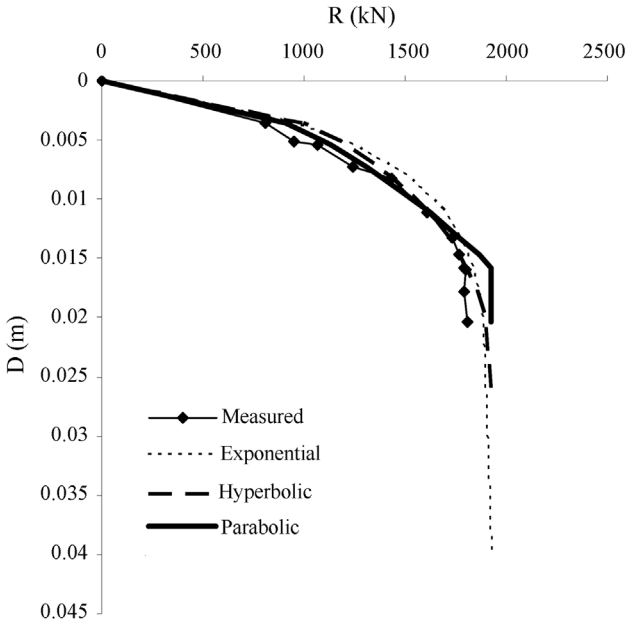

Figure 8 - Comparison of the measured and calculated *R vs. D* curves.

The data captured by the sensors fastened onto the piles were processed by the simplified CASE method and so obtaining *R*. The values of the soil damping coefficients of the CASE method (J_c) were obtained with the greater energy blow in each test, by a numerical analysis using the CAPWAP (Case Pile Wave Analysis Program) method. This J_c value was used to all blows of that test.

Complementary details, such as the values of the weights of the pile-driving hammers used in the test, the PDA (Pile Driving Analyzer) model used, the pile age (time elapsed from pile installation and test date), the J_c values adopted in the test analyses, the values for fall heights (H_{fall}) of the hammer during the test, the maximum displacement in each hammer blow (*D*) measured in the test, the values for mobilized static resistances (*R*) calculated by the CASE method, and the values of maximum kinetic energy (*T*) transferred to the pile, using the value of EMX given by the dynamic load test, can be found in Alves (2010).

All of the piles were made from precast reinforced concrete with metal splices at the ends. The concrete presented characteristic resistance (f_{ck}) of 35 MPa. When necessary, the splices of the elements were welded.

Table 3 shows the values for total length (L_{total}), driven length (*Lc*), diameter, section area, and dynamic modulus of elasticity of the structural elements of the studied piles.

The 21 tested piles were part of 12 different works in 7 Brazilian cities.

Free-fall pile drivers were used in all tests, with steel hammers weighting from 18.5 to 50 kN. The driving systems were equipped with a damping system that was composed of a metal helmet with a hardwood block and plywood cushion.

6.2. Comparison of different fit equations for extrapolation of the R *vs.* D curve

Table 4 shows the correlation coefficient values (R^2) of the three functions: exponential, hyperbolic, and para-

Table 3 - Geometric data of the piles.

Pile	L_{total} (m)	*Lc* (m)	Diam. (m)	Section area (m^2)	Dynamic Pile Elast. Modulus (GPa)
1	16.00	15.4	0.23*	0.04	26.0
2	15.80	14.1	0.50	0.13	26.1
3	7.00	4.5	0.40	0.08	25.6
4	8.00	5.8	0.27*	0.05	42.9
5	22.00	21.4	0.27*	0.05	26.1
6	11.00	9.6	0.42	0.09	31.7
7	12.00	8.7	0.42	0.09	31.7
8	13.00	11.5	0.33	0.06	26.1
9	14.00	12.5	0.33	0.06	26.1
10	12.90	11.2	0.33	0.06	26.1
11	12.00	10.1	0.42	0.09	26.1
12	9.00	6.0	0.38	0.06	26.1
13	18.00	17.2	0.42	0.09	26.1
14	14.15	7.3	0.40	0.08	25.6
15	7.00	5.5	0.40	0.08	25.6
16	7.00	5.7	0.27*	0.07	42.9
17	8.00	6.5	0.27*	0.07	42.9
18	20.00	18.7	0.27*	0.07	26.1
19	12.00	10.1	0.42	0.09	31.7
20	13.00	11.0	0.38	0.06	30.0
21	11.50	10.35	0.30	0.07	25.6

(*) = dimension of the side of the piles of square sections.

Table 4 - R^2 values of the exponential, hyperbolic, and parabolic functions.

Pile	Values of R^2		
	Exponential	Hyperbolic	Parabolic
1	0.935	**0.948**	0.776
2	**0.975**	0.913	0.880
3	**0.983**	0.943	0.919
4	0.925	**0.968**	0.556
5	**0.929**	0.827	0.888
6	**0.962**	0.944	0.913
7	**0.968**	0.884	0.856
8	**0.923**	0.901	0.769
9	**0.824**	0.679	0.719
10	**0.379**	0.175	0.151
11	**0.954**	0.908	0.925
12	0.818	0.784	**0.859**
13	**0.931**	0.929	0.918
14	**0.966**	0.880	0.867
15	0.899	0.877	**0.936**
16	0.541	**0.670**	0.378
17	0.374	0.520	**0.714**
18	**0.891**	0.820	0.856
19	0.818	0.784	**0.859**
20	**0.851**	0.657	0.675
21	0.756	0.721	**0.787**
Mean	**0.923**	0.877	0.856
Standard Deviation	**0.180**	0.190	0.200

bolic curves targeting the best fit for all of the pile load tests. The R^2 values in bold face are the ones that presented, among the three functions, the value closest to 1, *i.e.*, the function that presented the best fit in a particular pile.

It was observed that in 13 of the 21 studied piles, the best fit function for the *R vs. D* curve was the exponential function. Only five piles had the best fit for the parabolic function, and three piles had the best fit for the hyperbolic function.

Three tests call the attention in Table 4 by the lowest values of R^2. Test 10 presented a sudden rupture and tests 16 and 17 still presented a "very linear" behavior in the last stage of the test. As said before, in this situations any extrapolation method is not efficient in predicting the ultimate static resistance, and this the reason for lower R^2 values.

Among the three studied functions, the mean of the R^2 values that presented the value closest to one was also the exponential function. Moreover, this function was shown to have the lowest standard deviation of the studied functions.

6.3. Different ultimate load criteria applied in the *R vs. D* curves

The dynamic increasing energy tests were used in this analysis. The tests were conducted until the point of pile-soil rupture, however, to use the rupture criteria to estimate the R_u, only the results obtained after one hammer blow before pile rupture were considered. The piles (listed in Table 3) used in the present comparison were 02, 10, 11, 18, 20, and 21 because they mobilized the ultimate static resistance.

To compare the proposed method (SEM-CASE method), Table 5 presents the ratio of calculated R_u to measured R_u for the conventional methods that are usually applied for static load testing – SLT. All predictions were made using the same "*R vs. D*" curve measured in the dynamic increasing energy test.

Table 5 - Values of the ratio of calculated R_u to measured R_u for the extrapolation criteria of R_u for SLT and the SEM-CASE method of Piles 2, 10, 11, 18, 20,and 21.

Criterion/Pile	R_u Calculated/ R_u Measured					
	2	10	11	18	20	21
Van der Veen (1953)	1.154	1.001	1.078	1.082	1.204	1.008
80% Brinch Hansen (1963)	0.888	0.809	0.956	N/A	N/A	N/A
90% Brinch Hansen (1963)	0.999	0.91	1.076	N/A	N/A	N/A
Chin (1970)	1.462	1.107	1.389	N/A	2.564	1.344
Mazurkiewicz (1972)	1.07	1.024	1.097	1.111	N/A	1.083
Massad (1986)	1.066	1.452	1.139	1.544	1.573	1.074
Décourt (1996)	1.446	0.929	1.399	N/A	2.483	N/A
SEM-CASE	**1.042**	**1**	**1.004**	**1.042**	**1.043**	**1.025**

N/A = not available.

Figure 9 shows a 3D bar graph comparing all of the criteria shown in Table 5. It shows that the SEM-CASE method had the lower variation in the ratio of calculated R_u to measured R_u. The SEM-CASE presented a better prediction to all piles with relations "calculated/measured" very close to one. The predictions using the criteria of Van der Veen (1953), Brinch Hansen (1963) and Mazurkiewicz (1972) had a good behavior to this set of piles. The methods of Chin (1970), Massad (1986) and Décourt (1996) presented a higher variability, overpredicting in most of the cases.

7. Conclusions

This paper presents a new method, the Simplified Extrapolation Method of the Simplified CASE Method (SEM-CASE), to extrapolate the mobilized static resistance (R) *vs.* maximum displacement (D) behavior based on the complementary energy criterion. This method is mainly applicable to precast concrete piles and was calibrated with dynamic increasing energy tests.

With respect to the presented analyses, the following should be noted:

- The SEM-CASE method can be easily used and has an acceptable theoretical basis.
- The estimated values of the ultimate static resistance, obtained by the SEM-CASE method, were similar to the measured values, with an error below 10%.
- By evaluating three different functions (exponential, hyperbolic, and parabolic functions) to reach the best fit with the test, it was noted that the exponential function obtained better results in more than 60% of analyzed cases.

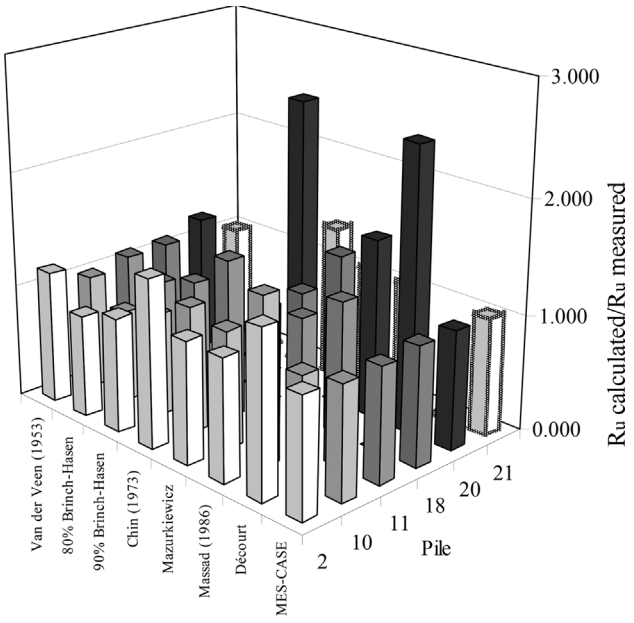

Figure 9 - Bargraph of the ratios of calculated R_u to measured R_u for all compared methods.

- The ability of classical methods to predict the ultimate load in static load tests was compared with the proposed SEM-CASE method. In the six presented dynamic load tests, the SEM-CASE resulted in better predictions that were closer to the ultimate measured resistance.
- The presented method was tested with a set of concrete driven piles. However, the same concept is surely valid for steel piles, since load tests on these piles normally present a well defined static resistance (R).
- As any other extrapolation method, the SEM-CASE method is applicable to tests that are gradually converging to the ultimate static resistance with a well-defined vertical asymptote.

Acknowledgments

The authors of this paper would like to thank the company SETE, Serviços Técnicos de Engenharia Ltd. for sharing the dynamic load tests used in this study, AGETOP, Agência Goiana de Transporte e Obras for its support, and CNPq, Conselho Nacional de Desenvolvimento Científico e Tecnológico for the financial support.

References

Alves, E.C. (2010). A New Extrapolation Method of Dynamic Load Tests: SEM-CASE. MSc Dissertation, School of Civil and Environmental Engineering. Federal University of Goias, Brazil, 250 p. (in Portuguese).

Aoki, N. (1989a). A new dynamic load test concept. Proc. 12th Int. Conf. on Soil Mechanics and Foundation Eng., ISSMFE, Rio de Janeiro, Session 14, Drivability of Piles. Japanese Society for Soil Mechanics and Foundation Engineering, Tokyo, v. 1, pp. 1-4.

Aoki, N. (1989b). Prediction of the behavior of vertical driven piles under static and dynamic conditions. Proc. 12th Int. Conf. on Soil Mechanics and Foundation Eng., ISSMFE, Rio de Janeiro, v. 2, pp. 56-61.

Aoki, N. (1997). Deformation of Ultimate Load Capacity of Driven Piles in Dynamic Increasing Energy Test. PhD Thesis, School of Civil Engineering, University of São Paulo, Brazil, (in portuguese).

Aoki, N. (2000). Improving the reliability of pile bearing capacity prediction by the dynamic increasing energy test (DIET). Proc. 6th Int. Conf. on the Application of Stress Wave Theory to Piles, São Paulo, pp. 635-651.

Brinch Hansen, J. (1963). Discussion: Hyperbolic stress-strain response: cohesive soils. American Society of Civil Engineers, J. of the Soil Mechanics and Foundation Div., 89(4):241-242.

Chin, F.K. (1970). Estimation of the ultimate load of piles not carried to failure. Proc. 2nd Southeast Asian Conference on Soil Engineering, pp. 81-90.

Clough, R.W. & Penzien, J. (1975). Dynamics of Structures. McGraw-Hill, New York.

Décourt, L. (1996). Evaluation of foundation rupture based on the concept of stiffness. Proc. III Seminário de Fundações Especiais, São Paulo-SP, Anais. ABMS, v. 2, pp. 215-224, (in Portuguese).

Hussein, M.H. & Goble, G.G. (2004). A brief history of the application of stress-wave. Theory to piles. Current Practices and Future Trends in Deep Foundations, Geotechnical Special Publication N. 125, ASCE, Reston, pp. 186-201.

Likins, G.E. & Rausche, F. (1981). Case method. The Second Seminar on the Dynamics of Pile Driving in Boulder, CO, Pile Dynamics, Inc., Cleveland, OH.

Likins, G.E.; Piscsalko, G.; Roppel, S. & Rausche, F. (2008). PDA testing: State of the art. Proc. 8th Int. Conf. on the Application of Stress Wave Theory to Piles, pp. 395-402.

Massad, F. (1986). Notes on the interpretation of failure load from routine pile loads tests. Soils and Rocks, 9(1):33-36.

Mazurkiewicz, B.K. (1972). Test Loading of Piles According to Polish Regulations. Royal Swedish Academy of Eng. Sciences, Committee on Pile Research, Report n. 35, Stockholm, 20 p.

Rausche, F., Goble, G.G. & Likins, G.E. (1985). Dynamic determination of pile capacity. ASCE Journal of Geotechnical Engineering, 111(3):367-383.

Smith, E.A.L. (1960). Pile driving analysis by the wave equation. J. Soil Mech. Found. Eng. Div., ASCE, 86(4):35-61.

Teferra, W.; Thendean, G. & Likins, G.E. (1996). Driving stress control during the installation of precast prestressed cylindrical concrete piles. Proc. 5th Int. Conf. on the Application of Stress-wave Theory to Piles, pp. 903-911.

Van der Veen, C. (1953). The bearing capacity of a pile. Proc. 3rd Int. Conf. on Soil Mechanics and Foundation Eng., Zurich, v. 2, pp. 84-90.

Warrington, D.C. (1997). Closed Form Solution of the Wave Equation for Piles. MSc Thesis, University of Tennessee at Chattanooga.

List of Symbols

a, b, c: parameters of regressions
A: cross-sectional area of pile
c: velocity of wave propagation
CAPWAP: Case Pile Wave Analysis Program
D, D_1, D_2: displacement
D_u: maximum displacement
DIET: dynamic increasing energy test
E: elastic modulus of pile material
Ft_1, Ft_2: values of forces
H_{fall}: fall heights of the hammer
J_c: dynamic damping coefficient
Lc: pile driven length
L_{total}: pile total length
PDA: Pile Driving Analyzer
R, R_1: mobilized static resistance
R_u: maximum resistance
R^2: values of correlation coefficient
S_u: maximum permanent penetration
t_1, t_2: time
T: total kinetic energy in the system
T_c: complementary kinetic energy
T_{cu}: maximum complementary kinetic energy
T_u: maximum kinetic energy
vt_1, vt_2: values of velocity
V: potential energy in the system
V_c: complementary potential energy
V_{cu}: maximum complementary potential energy
V_e: elastic strain energy
V_s: potential energy
W: work
W_{au}: work of the final damping forces
W_{nc}: work done by non conservatives forces
α: curve shape coefficient
δ: variation in the time interval (t_2-t_1)
ΔD, ΔD_1, ΔD_2: displacement increment or variation
ΔR : resistance variation
ΔV, ΔV_1, ΔV_2: energy variation

Appendix: Calculation of Complementary Energy When Using Different Fit Equations

As different fit equations could be used to represent the mobilized static resistance (R) *vs.* Displacement (D) curve, as shown in Fig. 2, this appendix explain how the complementary energy (V_c) is calculated in the three used functions in this paper: exponential, hyperbolic, and parabolic functions.

A) Exponential function

Based in Van der Veen (1953), Aoki (2000) proposed to express R x D relationship as:

$$R = R_u(1 - e^{-(\alpha D)}) \tag{20}$$

where R_u is the maximum resistance and α is a curve shape coefficient.

The potential energy (V_s) would be the integral of Eq. 20 from the origin to a generic value of "D":

$$V_s = \int_0^D R_u(1 - e^{-(\alpha D)})dD = \int_0^D R_u\,dD - \int_0^D R_u(e^{-(\alpha D)})dD \tag{21}$$

$$V_s = R_u\left[D - \frac{1}{\alpha}(1 - e^{-(\alpha D)})\right]. \tag{22}$$

The complementary energy can be calculated as:

$$V_c = RD - V_s. \tag{23}$$

Using the result of Eq. 22 in Eq. 23, results:

$$V_c = RD - R_u D + \frac{R_u}{a}(1 - e^{-(\alpha D)}) \quad (24)$$

and changing the value of "R" by Eq. 20, results:

$$V_c = \left(\frac{R_u}{\alpha}\right)\left[1 - (1 + \alpha D)e^{-\alpha D}\right]. \quad (25)$$

When D tends to large values of displacement, the limit complementary energy (V_{cu}) can be expressed as:

$$V_{cu} = \frac{R_u}{\alpha}. \quad (26)$$

B) Hyperbolic function

Using a hyperbolic relation between R x D:

$$R = R_u \sqrt{1 - \left(1 - \frac{D}{D_u}\right)^2} \quad (27)$$

where R_u is the maximum resistance and D_u is maximum displacement

This equation could be rewritten in different form:

$$D = D_u \left(1 - \sqrt{1 - \frac{R^2}{R_u^2}}\right). \quad (28)$$

In this form, the complementary energy (V_c) would be the integral of Eq. 27 from the origin up to a generic value of resistance (R):

$$\begin{aligned} V_c &= \int_0^R D_u \left(1 - \sqrt{1 - \frac{R^2}{R_u^2}}\right) dR \\ &= D_u \int_0^R dR - D_u \int_0^R \sqrt{1 - \frac{R^2}{R_u^2}} dR \end{aligned} \quad (29)$$

or

$$V_c = D_u R - \frac{D_u}{R_u}\left[\left(\frac{R}{2}\sqrt{R_u^2 - R^2}\right) + \left(\frac{R_u^2}{2}\arcsin\left(\frac{R}{R_u}\right)\right)\right]. \quad (30)$$

Replacing R by R_u, the limit complementary energy (V_{cu}) can be expressed as:

$$V_{cu} = D_u R_u \left[1 - \frac{1}{2}\arcsin(1)\right] \quad (31)$$

or approximately:

$$V_{cu} = 0.215 D_u R_u. \quad (32)$$

C) Parabolic function

Using a parabolic function where D would be proportional to the square of R, the relationship could be expressed as

$$D = \frac{R^2}{R_u^2} D_u. \quad (33)$$

The complementary energy (V_c) would be the integral of Eq. 33 from the origin up to a generic value of resistance (R):

$$V_c = \frac{D_u}{R_u^2}\int_0^R R^2 dR = \frac{D_u R^3}{3R_u^2}. \quad (34)$$

Replacing R by R_u, the limit complementary energy (V_{cu}) can be approximately expressed as:

$$V_{cu} = \frac{D_u R_u}{3}. \quad (35)$$